

Improvement of phase change behavior in titanium-doped $\text{Ge}_2\text{Sb}_2\text{Te}_5$ films

ZHANG Ying¹, WEI Shen-Jin¹, YI Xin-Yu¹, CHENG Shuai¹,
CHEN Kun¹, ZHU Huan-Feng¹, LI Jing^{1,2,3,*}, LV Lei⁴

- (1. Department of Optical Science and Engineering, Fudan University, Shanghai 200433, China;
2. Shanghai Engineering Research Center of Ultra-Precision Optical Manufacturing, Fudan University, Shanghai 200433, China;
3. Key Laboratory of Micro and Nano Photonic Structures (Ministry of Education), Fudan University, Shanghai 200433, China;
4. Department of Medical Physics, Weifang Medical University, Weifang 261053, China)

Abstract: The influence of Ti dopant in the titanium-doped $\text{Ge}_2\text{Sb}_2\text{Te}_5$ film upon its optical and structural characteristics has been investigated by spectroscopic ellipsometry and x-ray diffraction. Temperature-dependent resistance tests have further revealed that Ti-doped $\text{Ge}_2\text{Sb}_2\text{Te}_5$ films have better thermal stability than undoped one. Based on the Arrhenius extrapolation results from data retention tests, the endurance temperature corresponding to 10-year data retention of a Ti-doped $\text{Ge}_2\text{Sb}_2\text{Te}_5$ cell is higher than that of a common $\text{Ge}_2\text{Sb}_2\text{Te}_5$ cell without dopant. All these experimental results have confirmed that the Ti-doped $\text{Ge}_2\text{Sb}_2\text{Te}_5$ films are more suitable for the application in phase-change random access memory.

Key words: Ti-doped $\text{Ge}_2\text{Sb}_2\text{Te}_5$ films, phase-change behavior, thermal stability, data retention performance

PACS: 61.72.Vv, 81.15.Cd, 78.66.-w, 64.70.Kb

钛掺杂对 $\text{Ge}_2\text{Sb}_2\text{Te}_5$ 薄膜相变特性的改善

张颖¹, 魏慎金¹, 易歆雨¹, 程帅¹, 陈坤¹, 朱焕锋¹, 李晶^{1,2,3,*}, 吕磊⁴

- (1. 复旦大学光科学与工程系, 上海 200433; 2. 上海超精密光学制造工程技术研究中心, 上海 200433;
3. 复旦大学(教育部)微纳光子结构重点实验室, 上海 200433; 4. 潍坊医学院医学物理系, 山东 潍坊 261053)

摘要: 利用椭圆光谱术与 XRD 对钛掺杂 $\text{Ge}_2\text{Sb}_2\text{Te}_5$ 薄膜中钛元素对体系的光学性质及其微结构的影响进行了实验研究. 进而对该薄膜进行变温阻抗实验表明, 钛掺杂 $\text{Ge}_2\text{Sb}_2\text{Te}_5$ 薄膜与未掺杂的薄膜相比具有更好的热稳定性. 基于对薄膜样品的数据保持能力测试的实验数据, 经阿伦纽斯外推处理可知, 钛掺杂 $\text{Ge}_2\text{Sb}_2\text{Te}_5$ 薄膜样品的 10 年数据保持温度要高于未掺杂 $\text{Ge}_2\text{Sb}_2\text{Te}_5$ 薄膜样品. 本文的实验结果均证实, 钛掺杂 $\text{Ge}_2\text{Sb}_2\text{Te}_5$ 薄膜更适合应用于相变随机存取存储器中.

关键词: 钛掺杂 $\text{Ge}_2\text{Sb}_2\text{Te}_5$ 薄膜; 相变特性; 热稳定性; 数据保持能力

中图分类号: O484 文献标识码: A

Introduction

In normal conditions, the $\text{Ge}_2\text{Sb}_2\text{Te}_5$ (GST) thin film is one of the most promising materials for data-stor-

age applications because it can be switched reversibly between the amorphous and crystalline phases rapidly. It can be utilized to store information that the differences of optical reflectivity or electrical resistivity between the two states^[1-2]. Both phase-change optical disk and phase-

Received date: 2015 - 03 - 18, **revised date:** 2015 - 09 - 30

收稿日期: 2015 - 03 - 18, **修回日期:** 2015 - 09 - 30

Foundation items: Supported by Natural Science Foundation of Shanghai (13ZR1402600), National Natural Science Foundation of China (60578047), the National "973" Program of China (2012CB934303, 2009CB929201), Shanghai Commission of Science and Technology (06DJ14007), National "02" Project of China (2011ZX02402), and Natural Science Foundation of Shandong Province (2011ZRFL019)

Biography: ZHANG Ying (1987-), male, Chengdu, China, master degree. Main research areas are optical storage, preparation and physical properties of thin film materials.

* **Corresponding author:** E-mail: lijing@fudan.edu.cn

change random access memory (PRAM) have been successfully applied to data storages. However, it still holds the problems to be improved, including poor thermal stability and relatively high reset current that limit the practical application of a GST core cell in PRAM devices^[3-4]. During the past few years, great efforts have been made by doping different elements such as Ag^[5-6], Al^[7], N^[8], Ti^[9], O^[10], Zn^[11] and *etc.* into the conventional GST film in order to improve its phase change properties and performances.

As an important functional layer, the Ti adhesion layer or the TiN electrode are widely adopted in a PRAM cell. The problem is that a few of Ti element might diffuse into the GST core cell gradually through interfaces during recording/reading circulations, and they will affect the storage performance directly. Therefore, it is necessary to make clear influences on the phase change behavior of the GST core cell after Ti penetration. In this letter, the titanium-doped GST ($\text{Ti}_x\text{GST}_{1-x}$) thin films were deposited using co-sputtering method, and were investigated on the optical, structural, thermal and electrical properties of them.

1 Experimental results and discussions

Three different components of $\text{Ti}_x\text{GST}_{1-x}$ films have been deposited on thermal oxidation of silicon substrates by the direct-current (DC) co-sputtering method using the $\text{Ge}_2\text{Sb}_2\text{Te}_5$ and Ti targets in a working pressure of 3.5×10^{-3} mbar at room temperature. For comparison, the undoped GST films have been prepared using the $\text{Ge}_2\text{Sb}_2\text{Te}_5$ target only. A set of $\text{Ti}_x\text{GST}_{1-x}$ films is selected to analyze the dopant concentrations by the X-ray photoelectron spectroscopy (XPS), and the Ti concentrations are determined to be 4.6 at.% for the sample TiGST01, 4.1 at.% for the sample TiGST02 and 2.6 at.% for the sample TiGST03, respectively, and the undoped GST film is named the sample GST04. The film thicknesses of the samples TiGST01, TiGST02, TiGST03 and GST04 are 218 nm, 212 nm, 203 nm and 200 nm, respectively. Then, all of the samples have been performed thermal treatment in nitrogen ambient at different temperatures of 150°C, 250°C and 350°C for 1 minute separately. After annealing, the microstructure changes of the samples were characterized by the X-ray diffraction (XRD). Scanning range of the diffraction angle is set from 20.0° to 50.0° with the step of 0.02°.

Optical properties of the annealed and as-deposited $\text{Ti}_x\text{GST}_{1-x}$ films, as shown in Fig. 1, including (a) as-deposited samples, as well as the samples annealed at (b) 150°C, (c) 250°C and (d) 350°C for 1 min under the nitrogen ambient, were obtained from the analysis of spectroscopic ellipsometry data in the spectral region from 300 nm to 800 nm.

According to our experimental results, the extinction coefficient k curve of a GST sample goes up monotonously while annealing temperature increases, thus the change of crystallinity in the sample film is indirectly reflected by the changes in the k curve. As shown in Fig. 1(a), the extinction coefficient k differences of all the as-deposited films are not obvious. After annealing treatment at 150°C, the k curves of samples TiGST01 and TiGST02 in

Fig. 1(b) have almost no change compared with that of in Fig. 1(a). It indicates that they remained amorphous

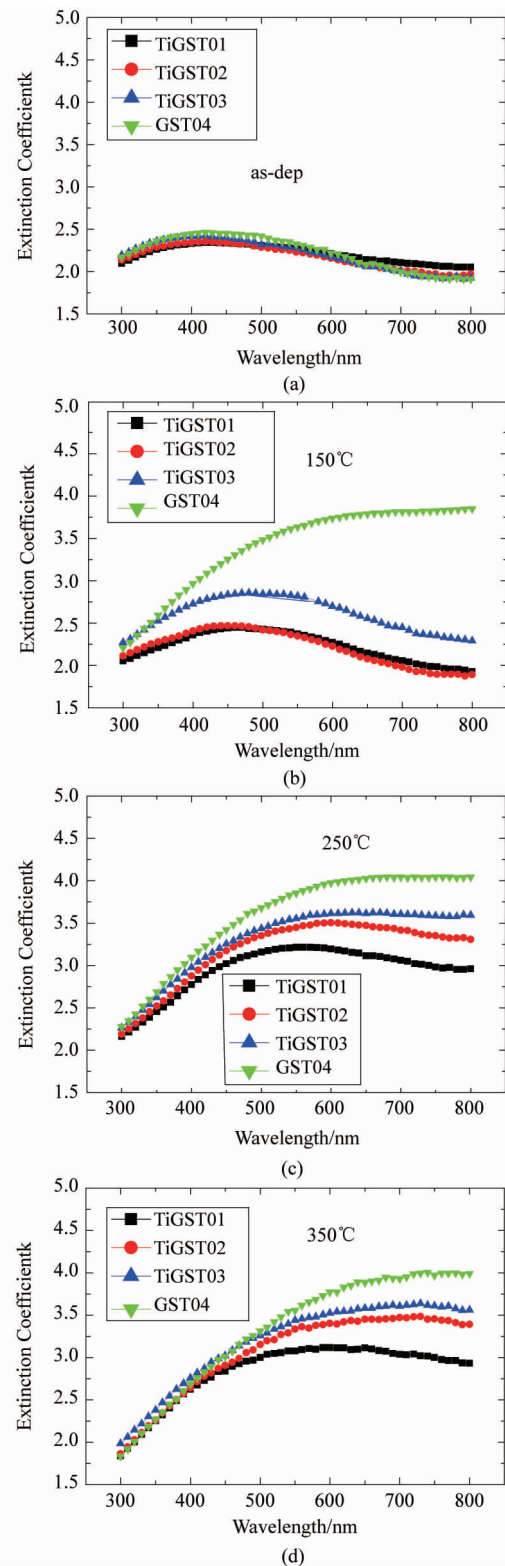


Fig. 1 Extinction coefficients spectra of the $\text{Ti}_x\text{GST}_{1-x}$ films annealed at different temperatures of (a) as-deposited, (b) 150°C, (c) 250°C, and (d) 350°C

图1 不同温度退火的 $\text{Ti}_x\text{GST}_{1-x}$ 薄膜的消光系数(a)沉积态, (b) 150°C, (c) 250°C, (d) 350°C

state due to the effect of Ti dopant with a certain concentration ratio. Apparently, the k curve of the sample TiGST03 film with the minimum Ti dopant goes up a lot compared with the as-deposited state itself, especially the k curve of the undoped sample GST04 does. Furthermore, in Fig. 1(c) and (d), the extinction coefficient k curves of the samples show the evident differences that the crystallinity of the sample films is enhanced gradually. In the meantime, with the increase of the Ti doping concentration, the crystallinity of the sample films decreases.

According to the extinction coefficient k of the samples, the optical band gap E_g can be determined from the power-law behavior of Tauc^[12] as follow:

$$(\alpha hv)^{1/2} = C(hv - E_g) \quad (1)$$

where α is the absorption coefficient, hv is the photon energy and C is a constant. The absorption coefficient can be calculated from the equation of $\alpha = 4\pi k/\lambda$.

Figure 2 shows the plot of the $(\alpha hv)^{1/2}$ vs curves for the sample films with different Ti doping at annealing temperature of 150°C. The optical band gap E_g is then determined by extrapolating the linear portion of the curves in the limit of $(\alpha hv)^{1/2} = 0$. All of the values of the optical band gap E_g are listed in Table 1. Obviously, it can be found that with the increase of annealing temperature, the optical band gaps decrease for the same titanium content of the samples, and increase with the increase of Ti doping at the same temperature. This is confirmed from another side that the transformation of crystallization is restrained by Ti doping.

In order to obtain the micro-structure information of the above samples, the x-ray diffraction (XRD) measurement has been adopted. According to Fig. 3(a), for the more Ti doped samples TiGST01 and TiGST02, there

Table 1 The optical band gaps of all samples at different annealing temperatures

表 1 所有样品在不同退火温度下的光学带隙

Temperatures/°C		TiGST01	TiGST02	TiGST03	GST04
as-dep.		0.76	0.76	0.66	0.65
150	Optical	0.75	0.75	0.56	0.40
250	band gap E_g	0.65	0.41	0.35	0.31
350	eV	0.43	0.34	0.31	0.30

are almost no XRD peaks. This indicates that these two Ti-doped films still remain amorphous state. However, a set of diffraction peaks corresponding to a NaCl-type face-centered cubic (fcc) structure appeared in the patterns of the samples TiGST03 and GST04, including fcc(200) and fcc(220) at about 29.6° and 42.8°, respectively. Until the sample GST04 annealed at 350°C in Fig. 3(c), the hexagonal close-packed (hcp) phase appears, but the Ti doped samples TiGST01, TiGST02 and TiGST03 remain still in fcc phase. Therefore, the Ti element doped into $\text{Ge}_2\text{Sb}_2\text{Te}_5$ matrix properly will restrain the transition from the amorphous state to the fcc phase, and from the fcc phase to the hcp phase as well.

Figure 3(b) shows the XRD patterns for the films annealed at 250°C. Obviously, the main characteristic fcc peaks appear in all of these samples, including fcc(200), fcc(220) and fcc(111), at 29.6°, 42.8° and

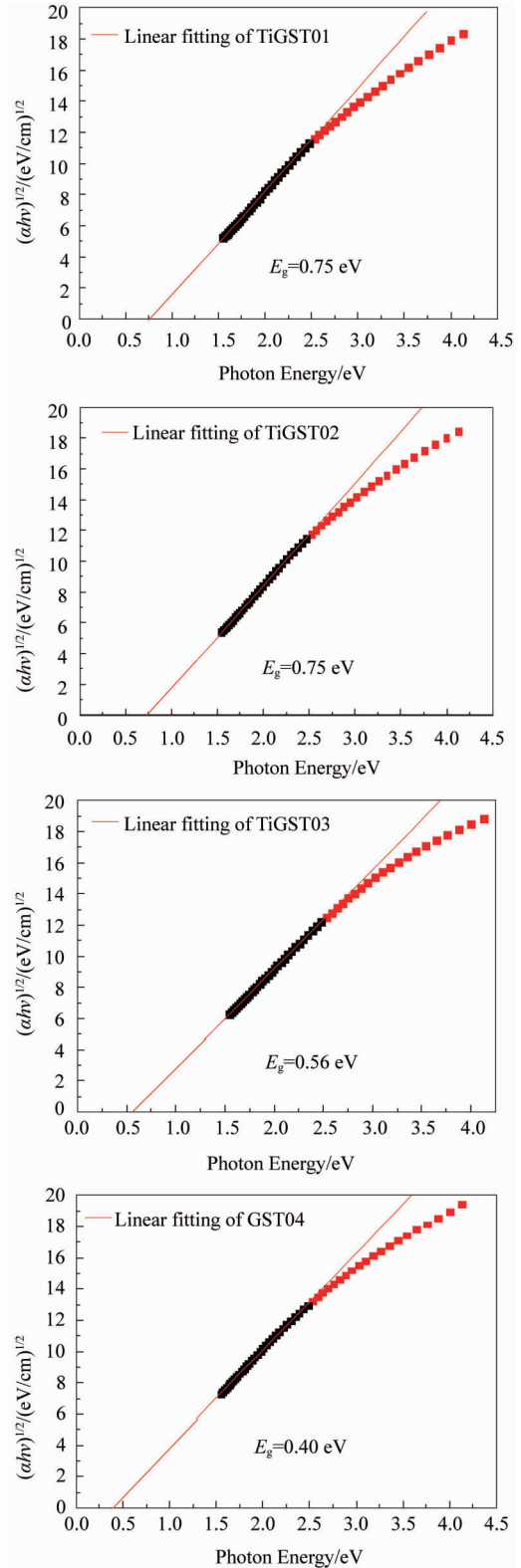


Fig. 2 The optical band gaps E_g of the $\text{Ti}_x\text{GST}_{1-x}$ films annealed at 150°C

图 2 150°C退火的 $\text{Ti}_x\text{GST}_{1-x}$ 薄膜的光学带隙

25.7°, respectively. It can also be found that the full width at half maximum (FWHM) is broadened as the amount of Ti increased, which indicates that the more Ti

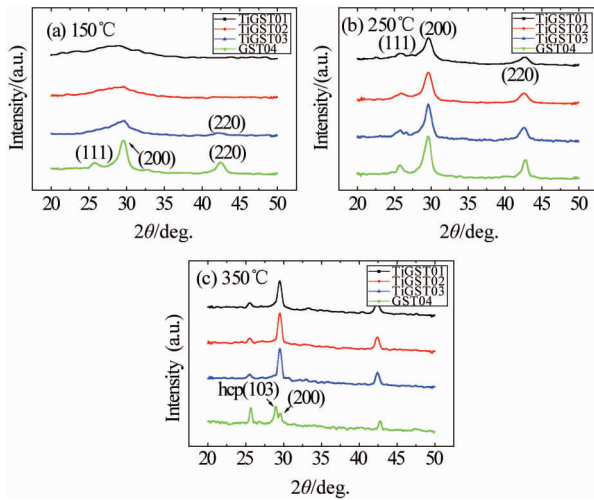


Fig. 3 XRD patterns of the Ti_xGST_{1-x} films annealed at (a) 150°C, (b) 250°C, and (c) 350°C

图3 不同温度退火的 Ti_xGST_{1-x}薄膜的 XRD 衍射图谱(a) 150°C, (b) 250°C, (c) 350°C

atoms doped, the more crystallinity restrained. The XRD results are in good agreement with the ellipsometry measurements above.

Moreover, Scherrer formula^[13] of $D = 0.89\lambda/\beta\cos\theta$ is adopted to estimate grain sizes of the films by using the FWHM of the (220) diffraction peak. The average results are 8 nm, 10 nm, 12 nm and 20 nm for the samples TiGST01, TiGST02, TiGST03 and GST04 in the (220) crystal orientation, respectively. Thus, the crystalline grain sizes in the Ti_xGST_{1-x} films decreased with the increase of Ti concentration at the same annealing temperature.

To obtain both the time-dependent resistance ($R-t$) and the temperature-dependent resistance ($R-T$) characteristics, a two-point-probe testing system is employed. The measurements have been performed under argon ambient in order to avoid oxidation during in situ thermal treatment.

As shown in Fig. 4, the resistance curves of all samples drop continuously with the increase of temperature. A steep drop of each resistance curve can be found at about 187°C, 172°C, 166°C and 154°C, respectively, which is due to the amorphous-to-fcc phase change. The Ti-doped films of the samples TiGST01, TiGST02 and TiGST03 had higher crystallization temperatures because their thermal stability can be enhanced gradually with the increase of Ti concentration. As the temperature continues to rise, the second steep drop appeared only in the resistance curve of the sample GST04 at about 310°C. This indicates that the fcc-to-hcp phase change occurred in the undoped film. All of the Ti-doped film samples were still in the fcc phase. Further experimental evidence confirmed that Ti doping can enhance their temperature stability of the Ti_xGST_{1-x} samples.

In addition, the experimental results have shown that the Ti-doped films have higher crystalline resistance than that of undoped GST film. The total grain boundary becomes large in the films because the grain size of the Ti_xGST_{1-x} samples can be reduced by doping Ti. Thus the

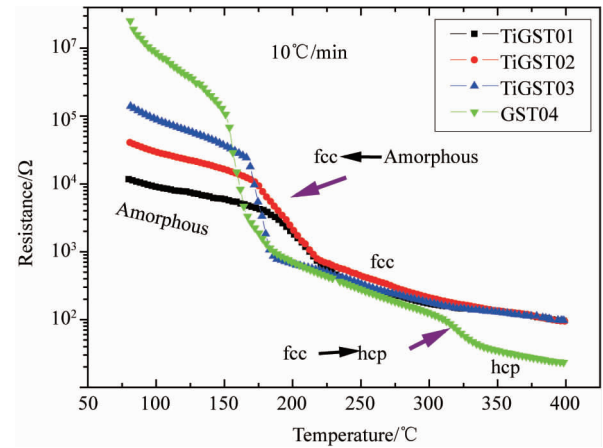


Fig. 4 Resistance curves changing with temperature at a rate of 10°C/min for the Ti_xGST_{1-x} films

图4 10°C/min 变温处理的 Ti_xGST_{1-x}薄膜的电阻变化曲线

carrier scattering is enhanced resulting in the increase of the crystalline resistance. Therefore it will increase the joule heat for the RESET operation corresponding to the fcc-to-amorphous phase change process in the storage application, when an identical electrical current is applied and less power is needed.

Meanwhile the Ti-doped films have lower amorphous resistances with the increase of Ti content because more free electrons are provided by the Ti dopant. However, there is still more than one order of magnitude difference in the resistance between two phases via appropriate regulation of Ti doping, which provides enough On/OFF ratio for PRAM devices.

Furthermore, in order to characterize the data retention capability of the samples, in-site resistance testing was taken in isothermal conditions while these films were heated in argon protection environment. When resistance value drops to the threshold resistance that is 50% of the initial value, the device is called data retention failure. According to the Arrhenius law^[14]:

$$\ln t = E_a/kT - \ln\tau \quad (2)$$

where t is the failure-time, E_a is the crystalline activation energy, k is Boltzmann's constant, T is the isothermal temperature, and τ is a proportional time constant. In the experiments, the failure-time t has been calculated by the average value of multiple measurements at certain fixed temperatures. The $\ln t$ via $1/T$ diagram by linear fitting is shown in Fig. 4.

In accordance with Fig. 5, the failure-temperature corresponding to 10-year data retention is 111°C, 103°C, 85°C and 82°C for the samples TiGST01, TiGST02, TiGST03 and GST04 respectively, with the crystalline activation energy of 3.09 eV, 2.81 eV, 2.76 eV and 2.67 eV for each homologous sample. These results have confirmed that the Ti-doped GST films have a better data retention capacity than undoped one.

2 Conclusions

In summary, the influence of Ti doping on the phase change characteristics of Ti_xGST_{1-x} films has been investi-

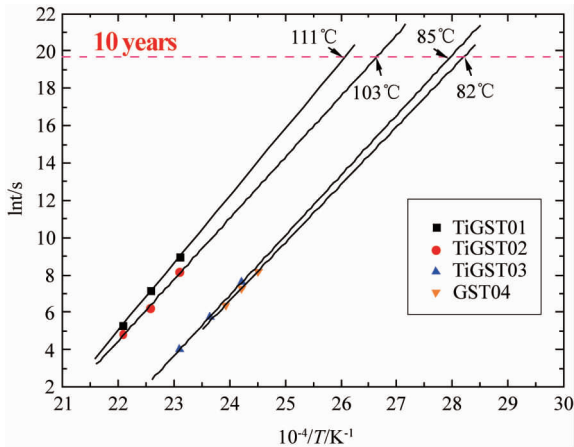


Fig.5 The failure temperature by the Arrhenius extrapolation of 10-year data retention for the $Ti_x GST_{1-x}$ films

图5 $Ti_x GST_{1-x}$ 薄膜数据保持十年对应的最高温度

gated carefully. The ellipsometry and XRD results have revealed that Ti dopant has a certain inhibiting effect on the crystallization of the $Ti_x GST_{1-x}$ samples, the higher of Ti doping concentration, the smaller the grain size. Furthermore, based on the temperature-dependent resistance experiments, the appropriate Ti-doped sample has higher crystallization temperature, which indicates that the sample has better thermal stability. High crystalline resistance is also useful for reducing the RESET current. In the meantime, the $Ti_x GST_{1-x}$ film with appropriate Ti dopant exhibits better data retention capability than that of undoped one. In general, it can be proved that the penetration of Ti ions from the TiN or Ti layers into the GST core cell will improve its thermal stability and endurance property on its performance in usual applications.

Acknowledgements

One of the authors (J. Li) acknowledges the financial supports by the Natural Science Foundation of Shanghai (No. 13ZR1402600), the National Natural Science Foundation of China (No. 60578047), the Na-

tional “973” Program of China (Nos. 2012CB934303, 2009CB929201), the Shanghai Commission of Science and Technology (No. 06DJ14007), the National “02” Project of China (No. 2011ZX02402), and the Natural Science Foundation of Shandong Province (No. 2011ZRFL019).

References

- [1] Ovshinsky S R. Reversible electrical switching phenomena in disordered structures [J]. *Phys. Rev. Lett.*, 1968, **21**:1450–1453.
- [2] Wuttig M, Yamada N. Phase-change materials for rewritable data storage [J]. *Nat. Mater.*, 2007, **6**: 824–832.
- [3] Sutou Y, Kamada T, Sumiya M, *et al.* Crystallization process and thermal stability of $Ge_1Cu_2Te_3$ amorphous thin films for use as phase change materials [J]. *Acta Mater.*, 2012, **60**: 872–880.
- [4] Ryu S W, Lee J H, Ahn Y B, *et al.* SiO_2 doped $Ge_2Sb_2Te_5$ thin films with high thermal efficiency for applications in phase change random access memory [J]. *Nanotechnology*, 2011, **22**: 254005.
- [5] Frumar M, Wagner T. Ag doped chalcogenide glasses and their applications [J]. *Curr. Opin. Solid State Mater. Sci.*, 2003, **7**: 117–126.
- [6] Song K H, Kim S W, Seo J H, *et al.* Influence of the additive Ag for crystallization of amorphous Ge-Sb-Te thin films [J]. *Thin Solid Films*, 2009, **517**(14): 3958–3962.
- [7] Wei S J, Li J, Wu X, *et al.* Phase change characteristics of aluminum doped $Ge_2Sb_2Te_5$ films prepared by magnetron sputtering [J]. *Opt. Express*, 2007, **15**(17): 10584–10590.
- [8] Kim S, Park J, Jung S. Excellent resistive switching in nitrogen-doped $Ge_2Sb_2Te_5$ devices for field-programmable gate array configurations [J]. *Appl. Phys. Lett.*, 2011, **99**:192110.
- [9] Wei S J, Zhu H F, Chen K, *et al.* Phase change behavior in titanium-doped $Ge_2Sb_2Te_5$ films [J]. *Appl. Phys. Lett.*, 2011, **98**: 231910.
- [10] Jang M H, Park S J, Lim D H, *et al.* Effects of oxygen incorporation in GeSbTe films on electrical properties and thermal stability [J]. *Appl. Phys. Lett.*, 2010, **96**: 092108.
- [11] Wang G X, Nie Q H, Shen X, *et al.* Phase change behaviors of Zn-doped $Ge_2Sb_2Te_5$ films [J]. *Appl. Phys. Lett.*, 2013, **101**: 051906.
- [12] Callaway J. *Quantum Theory of the Solid State* [M]. London: Academic Press. Inc., 1974.
- [13] Patterson A L. The Scherrer Formula for X-Ray Particle Size Determination [J]. *Phys. Rev.*, 1939, **56**: 978–982.
- [14] Kao K F, Lee C M, Chen M J, *et al.* $Ga_2Te_3Sb_5$ —A candidate for fast and ultralong retention phase-change memory [J]. *Adv. Mater.*, 2009, **21**: 1695–1699.